

TRANSVERSE MOMENTUM DISTRIBUTIONS FROM EFFECTIVE FIELD THEORY

Sonny Mantry*

*University of Wisconsin at Madison
 Madison, WI 53706, USA
 mantry147@gmail.com*

Frank Petriello

*High Energy Physics Division, Argonne National Laboratory
 Argonne, IL 60439, USA*

*Department of Physics & Astronomy, Northwestern University
 Evanston, IL 60208, USA
 f-petriello@northwestern.edu*

We review a new approach to calculating transverse momentum distributions of the Higgs and electroweak gauge bosons using the Soft-Collinear Effective Theory. We derive a factorization theorem for transverse momentum distributions in terms of newly-defined impact-parameter beam functions (iBFs) and an inverse soft function (iSF). The iBFs correspond to completely unintegrated parton distribution functions and provide interesting probes of momentum distributions within nucleons. The numerical matching between the low and high transverse momentum regions is improved in this approach with respect to standard techniques. We present results for next-to-leading logarithmic resummation for the Higgs and Z-boson distributions and give a comparison with Tevatron data.

1. Introduction

Low transverse momentum (p_T) distributions of the Higgs and electroweak gauge bosons play an important role in numerous physics studies, including Higgs searches, precision measurements of the W -boson mass, tests of perturbative QCD, and in probing transverse momentum dynamics in the nucleon. In the region $p_T \ll M$, where M denotes the mass of the Higgs or electroweak boson in question, large double logarithms in p_T/M spoil the convergence of the perturbative expansion in the strong coupling. A proper description of the transverse momentum distributions in this region requires resummation of these large logarithms. Extensive studies [1, 2, 3, 4, 5, 6, 7, 8, 9, 10, 11, 12, 13, 14, 15, 16] of low p_T resummation have

*Invited Talk presented at the workshop on “QCD Evolution of Parton Distributions: from Collinear to Non-collinear Case”, April 8th-9th, 2011, Thomas Jefferson National Accelerator Facility, Newport News, VA, USA.

been performed. Most are based on the well-known Collins-Soper-Sterman (CSS) formalism.

More recently in Refs. [17, 18, 19], low p_T resummation was studied using the Soft-Collinear Effective Theory (SCET) [20, 21, 22]. In the region $M \gg p_T \gg \Lambda_{QCD}$, the schematic form of the factorization theorem is

$$\frac{d^2\sigma}{dp_T^2 dY} \sim H \otimes \mathcal{G} \otimes f \otimes f. \quad (1)$$

Here, H is a hard function that encodes the physics of the hard production vertex and whose renormalization group (RG) evolution sums the logarithms of p_T/M . \mathcal{G} is a gauge invariant Transverse Momentum Function (TMF) at the scale $\mu_T \sim p_T$ that describes the dynamics of initial state soft and collinear emissions that recoil against the heavy boson. f denotes the standard PDF and is evaluated at $\mu_T \sim p_T$ as determined by DGLAP evolution. In the region where $p_T \sim \Lambda_{QCD}$, the TMF becomes non-perturbative and encodes the transverse momentum dynamics in the nucleons and of the soft radiation in the process.

A smooth transition between the regions of non-perturbative and perturbative p_T is achieved by implementing a model¹⁹ for the TMF \mathcal{G} in the non-perturbative region such that it has the correct RG evolution properties and smoothly reduces to the perturbative result for increasing p_T . The field-theoretic definition of \mathcal{G} provides further insight into the structure of the factorization theorem. In particular, we identify new objects called Impact-parameter Beam Functions (iBFs) which correspond to fully unintegrated PDFs. The form of the factorization in terms of these iBFs has differences compared to the more traditional TMDPDF formalism (see other proceedings [23, 24, 25] of this workshop for the most current overview). We give a brief discussion on this in the next section. In the following sections, we also give an overview of the factorization theorem, numerical results, and provide comparison with data.

2. Overview of Factorization Theorem

The first step in the derivation of the factorization theorem is to integrate out the hard production scale by matching QCD onto the SCET which describes the dynamics of initial state collinear and soft emissions that recoil against the heavy boson. These modes in the SCET have the momentum scalings

$$p_n \sim M(\eta^2, 1, \eta), \quad p_{\bar{n}} \sim M(1, \eta^2, \eta), \quad p_s \sim M(\eta, \eta, \eta), \quad \eta \sim \frac{p_T}{M}, \quad (2)$$

corresponding to the n -collinear, \bar{n} -collinear, and soft modes respectively. The heavy boson acquires finite transverse momentum by recoiling against these soft and collinear modes which have transverse momenta of order p_T . Using the soft-collinear decoupling property of the SCET, the dynamics of the collinear and soft emissions are separated into two zero-bin subtracted^{26,27} iBFs ($B_n, B_{\bar{n}}$) and a soft function (S) respectively. The zero-bin subtraction is necessary to avoid double counting the

soft region. Such a subtraction also appears in the TMDPDF formalism²⁸. Using the equivalence of the zero-bin and soft subtractions one can rewrite the factorization theorem in terms of iBFs ($\tilde{B}_n, \tilde{B}_{\bar{n}}$) defined without the soft zero-bin subtractions and an Inverse Soft Function (iSF). In the rest of this article, iBFs will refer to the $\tilde{B}_n, \tilde{B}_{\bar{n}}$ functions defined without the soft zero-bin subtraction. For perturbative values of the transverse momentum $p_T \gg \Lambda_{QCD}$, the iBFs are matched onto the standard PDFs after performing an operator product expansion in Λ_{QCD}/p_T . The Wilson coefficients of the iBF to PDF matching combined with the iSF give the TMF function \mathcal{G} . We schematically summarize these steps in deriving the factorization theorem below:

$$\begin{aligned}
 \frac{d^2\sigma}{dp_T^2 dY} &\sim \int PS |\mathcal{M}_{QCD}|^2 \\
 &\downarrow (\text{match QCD to SCET}_{p_T}) \\
 &\sim \int PS |C \otimes \langle \mathcal{O}_{SCET} \rangle|^2 \\
 &\downarrow (\text{SCET soft-collinear decoupling}) \\
 &\sim H \otimes B_n \otimes B_{\bar{n}} \otimes S \\
 &\downarrow (\text{zero-bin and soft subtraction equivalence}) \\
 &\sim H \otimes \tilde{B}_n \otimes \tilde{B}_{\bar{n}} \otimes S^{-1} \\
 &\downarrow (\text{iBF to PDF matching}) \\
 &\sim H \otimes \underbrace{[\mathcal{I}_n \otimes \mathcal{I}_{\bar{n}} \otimes S^{-1}]}_{\mathcal{G}} \otimes f_i \otimes f_j,
 \end{aligned} \tag{3}$$

where the coefficients $\mathcal{I}_{n,\bar{n}}$ arise from the iBF-to-PDF matching

$$\tilde{B}_n = \mathcal{I}_n \otimes f, \quad \tilde{B}_{\bar{n}} = \mathcal{I}_{\bar{n}} \otimes f. \tag{4}$$

For $p_T \gg \Lambda_{QCD}$, the iBFs, which correspond to fully unintegrated PDFs, describe the evolution of the initial state nucleons followed by their disintegration into a jet of collinear radiation that recoils against the heavy boson. Analogous beam functions are known to arise in other processes at hadron colliders [29, 30]. For $p_T \sim \Lambda_{QCD}$, a perturbative matching of the iBF onto the PDF is no longer valid. In fact, in this region, the iBFs and the iSF are non-perturbative. Eq.(4) should no longer be viewed as a perturbative matching but instead must be viewed as a definition of the new non-perturbative functions \mathcal{I}_n and $\mathcal{I}_{\bar{n}}$. Thus, the TMF function \mathcal{G} is non-perturbative for $p_T \sim \Lambda_{QCD}$. It encodes the transverse momentum dynamics within the nucleon and in the soft radiation that determines the p_T of the heavy boson.

For the sake of brevity, we focus most discussion here specifically for the case of the Z-boson p_T distribution. We refer the reader for details of the derivation, notation, and the case of Higgs boson distribution to Refs. [17, 18]. The factorization

theorem for the Z-boson distribution takes the form

$$\begin{aligned} \frac{d^2\sigma}{dp_T^2 dY} &= \frac{\pi^2}{N_c^2} \int_0^1 dx_1 \int_0^1 dx_2 \int_{x_1}^1 \frac{dx'_1}{x'_1} \int_{x_2}^1 \frac{dx'_2}{x'_2} \\ &\times H_Z^q(x_1 x_2 Q^2, \mu_Q; \mu_T) \mathcal{G}^{qrs}(x_1, x_2, x'_1, x'_2, p_T, Y, \mu_T) f_r(x'_1, \mu_T) f_s(x'_2, \mu_T), \end{aligned} \quad (5)$$

where the indices r, s run over the initial partons. The TMF function \mathcal{G}^{qrs} is given by

$$\begin{aligned} \mathcal{G}^{qrs}(x_1, x_2, x'_1, x'_2, p_T, Y, \mu_T) &= \int \frac{d^2 b_\perp}{(2\pi)^2} J_0[b_\perp p_T] \int dt_n^+ dt_{\bar{n}}^- \\ &\times \mathcal{I}_{n;q'r}(\frac{x_1}{x'_1}, t_n^+, b_\perp, \mu_T) \mathcal{I}_{\bar{n};\bar{q}s}(\frac{x_2}{x'_2}, t_{\bar{n}}^-, b_\perp, \mu_T) \\ &\times S_{qq}^{-1}(x_1 Q - e^Y \sqrt{p_T^2 + M_Z^2} - \frac{t_n^-}{x_2 Q}, x_2 Q - e^{-Y} \sqrt{p_T^2 + M_Z^2} - \frac{t_{\bar{n}}^+}{x_1 Q}, b_\perp, \mu_T). \end{aligned} \quad (6)$$

The iSF $S_{qq}^{-1}(\tilde{\omega}_1, \tilde{\omega}_2, b_\perp, \mu)$ is given by

$$S_{qq}^{-1}(\tilde{\omega}_1, \tilde{\omega}_2, b_\perp, \mu) = \int \frac{db^+ db^-}{16\pi^2} e^{\frac{i}{2}\tilde{\omega}_1 b^+} e^{\frac{i}{2}\tilde{\omega}_2 b^-} S_{qq}^{-1}(b^+, b^-, b_\perp, \mu) \quad (7)$$

where the position-space soft function $S_{qq}(b^+, b^-, b_\perp, \mu)$ is given by the vacuum matrix element of soft Wilson lines as

$$S_{qq}(b^+, b^-, b_\perp, \mu) = \text{Tr}\langle 0 | \bar{T}[S_n^\dagger S_{\bar{n}}](b^+, b^-, b_\perp) T[S_{\bar{n}}^\dagger S_n](0) | 0 \rangle. \quad (8)$$

The n-collinear iBF is defined as a nucleon matrix element of collinear quark fields and Wilson lines in SCET as

$$\begin{aligned} \tilde{B}_n^q(x, t, b_\perp, \mu) &= \frac{1}{2x \bar{n} \cdot p_1} \int \frac{db^-}{4\pi} e^{\frac{it}{2Qx} b^-} \langle p_1 | \bar{\xi}_{nq} W_n(b^-, b_\perp) \frac{\not{p}}{2} \\ &\times \delta(\bar{n} \cdot \mathcal{P} - x \bar{n} \cdot p_1) W_n^\dagger \xi_{nq}(0) | p_1 \rangle \end{aligned} \quad (9)$$

and the coefficients $\mathcal{I}_{n;q'r}$ appearing in Eq.(6) are given by the iBF to PDF matching equation

$$\begin{aligned} \tilde{B}_n^q(x, t, b_\perp, \mu) &= \int_x^1 \frac{dz}{z} \left\{ \mathcal{I}_{n;qq'}(\frac{x}{z}, t, b_\perp, \mu) f_{q'}(z, \mu) \right. \\ &\quad \left. + \mathcal{I}_{n;qg}(\frac{x}{z}, t, b_\perp, \mu) f_g(z, \mu) \right\}. \end{aligned} \quad (10)$$

Analogous equations exist for the \bar{n} -collinear functions.

As can be seen from Eq.(9), the iBF corresponds to a fully unintegrated PDF. This is in contrast with the TMDPDF which has been extensively studied in the context of transverse momentum distributions. The TMDPDF is typically defined with reference to an external regulator to regulate spurious rapidity divergences that arise in perturbative calculations. The independence of the cross-section from this external regulator gives rise to the Collins-Soper evolution equation which sums large logarithms. In contrast, the iBF is free of rapidity divergences. They are automatically regulated by the additional residual light-cone momentum component

(k^+) which appears through the definition of the convolution variable $t = Qk^+$. This is a reflection of the fact that for a finite p_T gluon recoiling against the heavy boson, the mass-shell condition $p^+p^- = p_T^2$ ensures a non-zero residual light-cone momentum component so that no rapidity divergence occurs in the physical process. The use of the residual light-cone momentum component to regulate rapidity divergences differs from the TMDPDF approach where an external regulator is introduced instead. The iBF is more differential than the TMDPDF and corresponds to a fully unintegrated PDF. A more detailed understanding of the relationship between the TMDPDF and the iBF approaches requires further study. However, an explicit comparison of the iBF approach with the TMDPDF or CSS formalism is possible by expanding the resummed results and comparing the logarithms generated at any fixed order in perturbation theory. Such an explicit check of the leading and next-to-leading logs in the iBF approach was performed in Ref. [18].

3. Numerical Results

In this section, we present numerical results for the Higgs boson and Z-boson p_T distributions. We refer the reader to Refs. [17, 18] for analytic expressions for the iBFs and the iSF. In Fig. 1, we show the fixed order, Leading-Log (LL), and Next-to-Leading Log (NLL) resummed results for Higgs production at $\sqrt{s} = 7$ TeV and zero rapidity for a Higgs mass of $m_h = 165$ GeV. The plot is cut off at $p_T = 3$ GeV so that the distribution is given entirely in terms of perturbatively calculable functions and the standard PDFs. Study of the distribution for non-perturbative values of p_T requires a model for the TMF function. We describe our modeling procedure later for the case of Z production. From Fig. 1, we see that the effect of the resummation is dramatic and changes the shape of the distribution. In particular, the $1/p_T^2$ singular behavior of the fixed result is brought under control by resummation.

Similarly, we present NLL resummation results for the Z-boson distribution for perturbative values of p_T in Fig. 2. Also given is a comparison with Tevatron data collected by the CDF and D0 collaborations [31, 32]. The plot in Fig. 2 is cutoff at $p_T \sim 1.75$ GeV. As seen, good agreement is found with the Tevatron data. A description of the Z-boson p_T spectrum in the region $p_T \sim \Lambda_{QCD}$ requires a model for the Z-boson TMF function.

In Ref. [19], a phenomenological study of TMF models was carried out. The guiding principles for the construction of TMF models include reproducing the correct RG evolution properties and requiring that the TMF model reduces to the perturbative result as one increases p_T . These principles are encoded by writing the the TMF as a convolution [33, 34, 35, 36] of the perturbative expression of the TMF with a non-perturbative model function as

$$\begin{aligned}
 \mathcal{G}^{qrs}(x_1, x_2, x'_1, x'_2, p_T, Y, \mu_T) &= \int_0^\infty dp'_T \mathcal{G}_{\text{part.}}^{qrs}(x_1, x_2, x'_1, x'_2, p_T \sqrt{1 + (p'_T/p_T)^2}, Y, \mu_T) \\
 &\times G_{\text{mod}}(p'_T, a, \Lambda),
 \end{aligned}
 \tag{11}$$

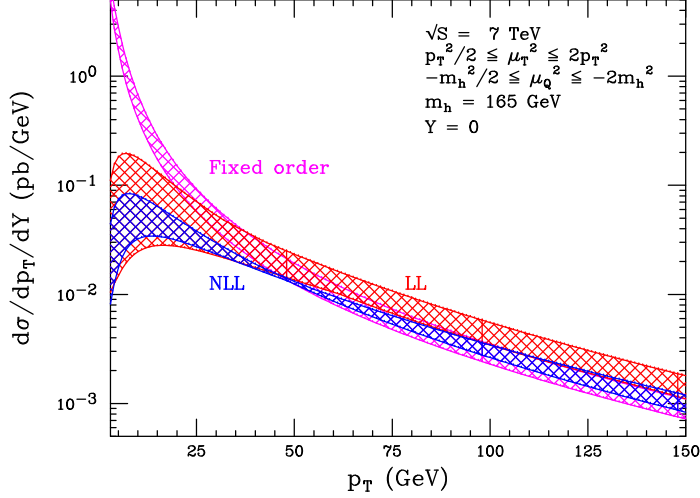


Fig. 1. Numerical predictions for the transverse momentum spectrum for Higgs boson production at the LHC for central rapidity. Shown are the fixed-order result and those obtained after implementing the resummation formula of Eq. (5) through LL and NLL. The bands arise from the scale variation.

where G_{mod} denotes a model function that peaks near $p'_T \sim \Lambda_{QCD}$ with parameters a, Λ that can be fit to data. The scale dependence of the TMF is contained entirely in the perturbative expression $\mathcal{G}_{part.}^{qrs}$ of the TMF so that the required RG evolution properties are reproduced. For phenomenological analysis we parameterize G_{mod} as

$$G_{mod}(p'_T, a, \Lambda) = \frac{2^{3/2-a}}{\Lambda} \frac{1}{\Gamma(a-1/2)} \left(\frac{p'^2_T}{\Lambda^2} \right)^{a-1} \exp\left[-\frac{p'^2_T}{2\Lambda^2}\right], \quad (12)$$

with the normalization condition

$$\int_0^\infty dp'_T G_{mod}(p'_T, a, \Lambda) = 1. \quad (13)$$

A sensible choice for μ_T that can be applied in both the perturbative and non-perturbative p_T regions is

$$\mu_T^2 = \xi^2 p_T^2 + p_{Tmin}^2, \quad (14)$$

where $p_{Tmin} > 1$ GeV is a low, but still perturbative, scale and can be viewed as another parameter of the model. ξ is a scale variation parameter we take to be $\mathcal{O}(1)$. The above choice of scale for μ_T has several useful properties. As $p_T \rightarrow 0$, the scale $\mu_T \rightarrow p_{Tmin}$ so that \mathcal{G}_{part}^{qrs} in Eq. (11) is still evaluated at a perturbative scale.

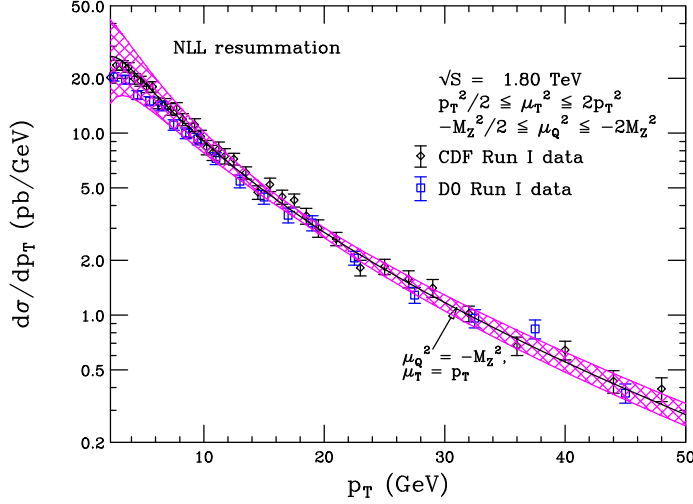


Fig. 2. Numerical predictions for the transverse momentum spectrum for Z boson production at Tevatron Run 1, compared with data from both CDF and D0. Shown is the resummation prediction at NLL accuracy. The bands arise from the scale variation, while the result for the central scale choice is shown by the solid line. The lower limit of the plot is $p_T = 1.75$ GeV.

Similarly, the running of the hard function $H_Z^q(x_1 x_2 Q^2, \mu_Q; \mu_T)$ will freeze at the perturbative scale p_{Tmin} as $p_T \rightarrow 0$. For larger values of $p_T \gg p_{Tmin}$, $\mu_T \rightarrow \xi p_T$ so that the appropriate choice of $\mu_T \sim p_T$ in the perturbative region is recovered. For $p_T \gg \Lambda_{QCD}$, the model TMF reduces to the expected perturbative expression up to power corrections as

$$\mathcal{G}^{qrs}(x_1, x_2, x'_1, x'_2, p_T, Y, \mu_T) \Big|_{p_T \gg \Lambda_{QCD}} = \mathcal{G}_{\text{part.}}^{qrs}(x_1, x_2, x'_1, x'_2, p_T, Y, \mu_T) + \mathcal{O}\left(\frac{\Lambda_{QCD}}{p_T}\right), \quad (15)$$

so that a smooth transition between the non-perturbative and perturbative regions is achieved. In Fig. 3, we show the Z -boson p_T spectrum including the non-perturbative p_T region. The values of the parameters $a = 2.50, \Lambda = 1.43$ GeV in G_{mod} used in Fig. 3, are obtained from a best fit to the CDF and D0 data for $p_T < 10$ GeV. We see that the form of the model TMF is flexible enough to describe data over the entire range of p_T .

4. Conclusions

We have presented a new factorization theorem for the low transverse momentum distributions of electroweak gauge and Higgs bosons using the SCET. The fac-

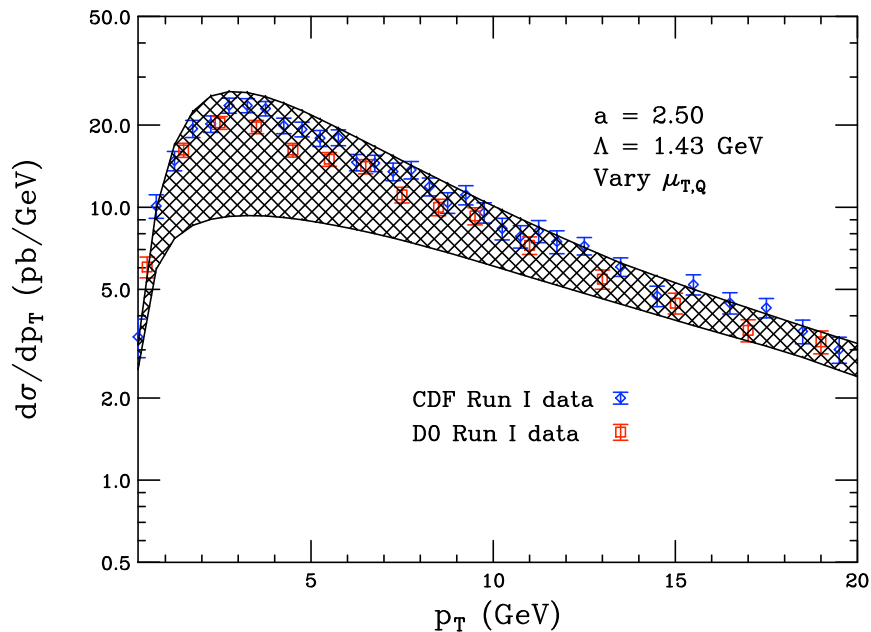


Fig. 3. The result for the p_T -spectrum of the Z-boson for the best fit parameter choices $a = 2.50, \Lambda = 1.43$ GeV. We have varied $\mu_{T,Q}$ within the range $1/2 < \xi_{T,Q} < 2$ for $\mu_T^2 = \xi_T p_T^2 + p_{Tmin}^2, \mu_Q^2 = -\xi_Q M_Z^2$ for $p_{Tmin} = 2$ GeV.

torization theorem is formulated in terms of Impact-parameter Beam Functions (iBFs) which correspond to fully unintegrated PDFs. We present results of NLL resummation for Higgs and Z-boson distributions. Good agreement is found with data collected by the CDF and D0 collaborations at the Tevatron. More work is in progress to achieve NNLL results; recently in Ref. [37], NNLO results for the soft function of the Z-boson p_T distribution were obtained. We look forward to the further development of our formalism and applications to phenomenology.

Acknowledgments

This work is supported in part by the U.S. Department of Energy, Division of High Energy Physics, under contract DE-AC02-06CH11357 and the grants DE-FG02-95ER40896 and DE-FG02-08ER4153, and by Northwestern University.

References

1. Y. L. Dokshitzer, D. Diakonov, and S. I. Troian, Phys. Lett. **B79**, 269 (1978).
2. G. Parisi and R. Petronzio, Nucl. Phys. **B154**, 427 (1979).
3. G. Curci, M. Greco, and Y. Srivastava, Nucl. Phys. **B159**, 451 (1979).
4. J. C. Collins and D. E. Soper, Nucl. Phys. **B193**, 381 (1981).
5. J. C. Collins, D. E. Soper, and G. Sterman, Nucl. Phys. **B250**, 199 (1985).
6. R. P. Kauffman, Phys. Rev. **D44**, 1415 (1991).
7. C. P. Yuan, Phys. Lett. **B283**, 395 (1992).
8. R. K. Ellis and S. Veseli, Nucl. Phys. **B511**, 649 (1998), hep-ph/9706526.
9. A. Kulesza, G. Sterman, and W. Vogelsang, Phys. Rev. **D66**, 014011 (2002), hep-ph/0202251.
10. E. L. Berger and J.-w. Qiu, Phys. Rev. **D67**, 034026 (2003), hep-ph/0210135.
11. G. Bozzi, S. Catani, D. de Florian, and M. Grazzini, Phys. Lett. **B564**, 65 (2003), hep-ph/0302104.
12. G. Bozzi, S. Catani, D. de Florian, and M. Grazzini, Nucl. Phys. **B737**, 73 (2006), hep-ph/0508068.
13. G. Bozzi, S. Catani, G. Ferrera, D. de Florian, and M. Grazzini, (2010), 1007.2351.
14. Y. Gao, C. S. Li, and J. J. Liu, Phys. Rev. **D72**, 114020 (2005), hep-ph/0501229.
15. T. Becher and M. Neubert, (2010), 1007.4005.
16. A. Idilbi, X.-d. Ji, and F. Yuan, Phys. Lett. **B625**, 253 (2005), hep-ph/0507196.
17. S. Mantry and F. Petriello, Phys. Rev. **D81**, 093007 (2010), 0911.4135.
18. S. Mantry and F. Petriello, Phys.Rev. **D83**, 053007 (2011), 1007.3773.
19. S. Mantry and F. Petriello, Phys.Rev. **D84**, 014030 (2011), 1011.0757.
20. C. W. Bauer, S. Fleming, D. Pirjol, and I. W. Stewart, Phys. Rev. **D63**, 114020 (2001), hep-ph/0011336.
21. C. W. Bauer, D. Pirjol, and I. W. Stewart, Phys. Rev. **D65**, 054022 (2002), hep-ph/0109045.
22. C. W. Bauer, S. Fleming, D. Pirjol, I. Z. Rothstein, and I. W. Stewart, Phys. Rev. **D66**, 014017 (2002), hep-ph/0202088.
23. J. Collins, (2011), 1107.4123, * Temporary entry *.
24. S. Aybat and T. Rogers, (2011), 1107.3973, * Temporary entry *.
25. I. Cherednikov and N. Stefanis, (2011), 1108.0811, * Temporary entry *.
26. A. V. Manohar and I. W. Stewart, Phys. Rev. **D76**, 074002 (2007), hep-ph/0605001.
27. A. Idilbi and T. Mehen, Phys. Rev. **D75**, 114017 (2007), hep-ph/0702022.
28. J. C. Collins and F. Hautmann, Phys.Lett. **B472**, 129 (2000), hep-ph/9908467.
29. S. Fleming, A. K. Leibovich, and T. Mehen, Phys. Rev. **D74**, 114004 (2006), hep-ph/0607121.
30. I. W. Stewart, F. J. Tackmann, and W. J. Waalewijn, Phys.Rev. **D81**, 094035 (2010), 0910.0467.
31. CDF, A. A. Affolder *et al.*, Phys. Rev. Lett. **84**, 845 (2000), hep-ex/0001021.
32. D0, B. Abbott *et al.*, Phys. Rev. Lett. **84**, 2792 (2000), hep-ex/9909020.
33. Z. Ligeti, I. W. Stewart, and F. J. Tackmann, Phys.Rev. **D78**, 114014 (2008), 0807.1926.
34. A. H. Hoang and I. W. Stewart, Phys.Lett. **B660**, 483 (2008), arXiv:0709.3519.
35. S. Fleming, A. H. Hoang, S. Mantry, and I. W. Stewart, Phys.Rev. **D77**, 074010 (2008), hep-ph/0703207.
36. S. Fleming, A. H. Hoang, S. Mantry, and I. W. Stewart, Phys.Rev. **D77**, 114003 (2008), arXiv:0711.2079.
37. Y. Li, S. Mantry, and F. Petriello, (2011), 1105.5171.